Glycobiology vol. 10 no. 7 pp. 691–700, 2000

Exploring the outcome of genetic modifications of glycosylation in cultured cell lines by concurrent isolation of the major classes of vertebrate glycans

Karin Norgard-Sumnicht, Xiaomei Bai, Jeffrey D.Esko, Ajit Varki[1] and Adriana E.Manzi[2]

Glycobiology Research and Training Center, Divisions of Hematology-Oncology and Cellular and Molecular Medicine, University of California, San Diego, La Jolla, CA 92093–0687, USA

Received on October 27, 1999; revised on January 18, 2000; accepted on January 28, 2000

In the preceding article (Manzi,A.E., Norgard-Sumnicht,K., Argade,S., Marth,J.D., van Halbeek,H. and Varki.A. [2000] *Glycobiology*, 10, 669–688), we reported a comprehensive approach for the extraction, fractionation, and isolation of all of the major classes of sugar chains (glycans) from vertebrate tissues. Here we apply this "Glycan Isolation Protocol" to a variety of cultured mammalian cell lines, including two wild-type Chinese hamster ovary (CHO) cell lines and some of their genetically modified variants that were predicted or known to have defined abnormalities in the biosynthesis of one or more classes of glycans. We also use this approach to characterize clone 489, a new derivative of the GAG-deficient CHO clone pgsA-745, in which sulfation has been restored by transfection of a wild-type CHO cDNA library. By metabolically labeling the cell lines with [6-^{3}H]glucosamine we were able to monitor the recovery of all major classes of glycans. The results allow us to reach several conclusions: first, the protocol described in the preceding paper is further validated by finding good recovery of total radioactivity and appropriate distribution of label in the correct glycan classes in the fractions from a variety of cell lines; second, the amount of radioactivity recovered in free glycosylphosphatidylinositol (GPI) lipids is remarkably high when compared to that found in GPI anchors, with the former being the dominant form in some cells; third, cells with known genetic mutations in specific glycosylation pathways are shown to have the expected changes in the distribution of recovered radioactivity in the appropriate fractions; fourth, the N- and O- glycans recovered via the protocol are of adequate quality to demonstrate marked differences in their structural profiles and/or content; fifth, the protocol can pick up unexpected differences of glycan classes not predicted to be affected by the primary defect; finally, the reappearance of sulfation in the novel clone 489 is not due to restoration of GAG sulfation, but rather due to the new expression of sulfation in the fraction enriched in N- and O-linked glycopeptides. These results demonstrate the power of this comprehensive approach for the concurrent exploration and profiling of the different major classes of glycans in cells.

Key words: biosynthesis/glycans/genetic modification/vertebrate

Introduction

Eukaryotic glycan biosynthesis involves several multienzymatic pathways that generate a diverse and complex array of structures (Schnaar, 1991; Ferguson, 1992; Furukawa and Kobata, 1992; Hart, 1992; Lis and Sharon, 1993; Margolis and Margolis, 1993; Hascall *et al.*, 1994; Hayes and Hart, 1994; Varki and Freeze, 1994; Hart, 1997; Weigel *et al.*, 1997). In much of the early work on glycan biosynthesis, glycosyltransferases were purified after detecting their activity using exogenous acceptors (Roseman, 1970; Sadler *et al.*, 1982; Stanley and Ioffe, 1995; Weigel *et al.*, 1997; Yeh and Cummings, 1997). Many cultured mammalian cell lines were also used over the years for studying the biosynthesis of particular classes of glycans. Some studies combined the use of metabolic radiolabeling of the glycans (Varki, 1994) with *in vitro* reactions, or with treatments of cells under different culture conditions and/or following addition of exogenous modulatory agents (Dinter and Berger, 1998). A variety of glycosylation mutants were also produced from such cells (Gottlieb *et al.*, 1974; Briles *et al.*, 1977; Stanley, 1984; Esko, 1986, 1989, 1991; Lidholt *et al.*, 1992; Stanley, 1992; Potvin *et al.*, 1995; Stanley and Ioffe, 1995; Bai and Esko, 1996; Stanley *et al.*, 1996; Bai *et al.*, 1999; Zhang *et al.*, 1999). Analysis of the altered glycans produced by these mutant or metabolically altered cells uncovered many *in vivo* substrate intermediates for known glycosyltransferase activities, and also led to the discovery of enzymes required in various biosynthetic pathways (Schachter, 1991; Van den Eijnden and Joziasse, 1993; Van den Eijnden *et al.*, 1995; Stanley *et al.*, 1996). While many of these approaches provided detailed information on the biosynthesis and metabolism of individual classes of glycans, limited attention was paid to the fate of other classes of glycans that might be affected by the treatments or the genetic changes imposed upon the cells. In fact, different classes of glycan chains share common sugar nucleotide precursors and, in some cases, common glycosyltransferases (Schachter, 1991; Van den Eijnden and Joziasse, 1993; Van den Eijnden *et al.*, 1995; Yeh and Cummings, 1997). Moreover, several glycosyltransferases compete with one another either for the same substrates or the same nucleotide donor in the subcompartments of the

[1]To whom correspondence should be addressed at: CMM-East, Room 1065, UCSD School of Medicine, La Jolla, CA 92093–0687

[2]Present address: Nextran Inc., An Affiliate of Baxter Healthcare Corporation, San Diego, CA

Table I. Radioactivity metabolically incorporated from [6-^{3}H]GlcN into four different cultured cell lines: distribution into different fractions obtained using the Glycan Isolation Protocol

Fraction	Predicted glycan content	% of total starting radioactivity			
		LS-180	MDCK	M-21	CHO-K1
PLE	GSLs, GIPLs	12.4	16.9	24.1	8.9
PLMW10	Monosaccharides and sugar nucleotides	13.7	6.6	8.9	14.8
SLMW3	Small glycopeptides	14.1	5.8	8.3	11.8
SLE	GPI anchors	6.6	5.9	5.4	3.1
GP0-100	N- and O-glycans	29.4	25.9	35.1	21.9
GP100–1000	GAGs and mucins	24.6	14.0	13.4	5.8
Total		100.8	75.1	95.2	66.3

Various cultured cell lines were metabolically labeled with [6-^{3}H]GlcN and the radioactivity was separated into different fractions using the Glycan Isolation Protocol. Aliquots were monitored at each step. The radioactivity in each fraction is presented as a percentage of the total amount of radioactivity in the starting material (cell extract plus matrix extract). See *Materials and methods* for the nomenclature of the fractions and the preceding manuscript for the predicted glycan content of each fraction.

Golgi apparatus (Abeijon *et al.*, 1997; Varki, 1998). The overall outcome of Golgi glycan biosynthesis thus reflects a delicate balance of several interacting pathways. However, there has so far not been a defined approach towards obtaining knowledge of the total glycan repertoire of cultured cell lines.

In the preceding article (Manzi *et al.*, 2000), we described a Glycan Isolation Protocol that permits the concurrent extraction and isolation of all the major classes of glycans from vertebrate tissues. Here we have further utilized this approach to analyze the glycosylation pattern of several commonly used cell lines, i.e., to obtain a typical glycoprofile for each cell line to determine the ratios of incorporated radioactivity in various subclasses of glycans. We have also studied several glycosylation mutants known to lack specific glycosyltransferases, and characterized the changes occurring in a new glycosylation variant of CHO cells.

Results and discussion

Concurrent isolation of the major classes of glycans from metabolically radiolabeled cells using the glycan isolation protocol

In the preceding article (Manzi *et al.*, 2000), we monitored recovery of radiolabeled standard glycans that were "spiked" into starting homogenates of whole mouse tissues. However, we could not directly demonstrate recovery of the corresponding unlabeled endogenous molecules in all the same fractions. As an alternative approach, we took advantage of the fact that metabolic labeling of cultured cells with [6-^{3}H]GlcN gives incorporation into GlcNAc, GalNAc and Sia, thereby introducing radioactivity into all the major classes of glycans (Varki, 1994). A variety of cultured cell lines were metabolically radiolabeled to "steady-state" through several doublings with this precursor, as described under *Materials and methods*. The washed cell pellets were combined with the labeled extracellular matrix recovered from the plates, and fractions predicted to contain the major classes of glycans were isolated, using the Glycan Isolation Protocol (Manzi *et al.*, 2000). Table I shows that the overall recovery of incorporated radioactivity among the different fractions with four different cell lines ranged from ~65–100% (because of variable quenching of radioactivity in different fractions, this is probably within the limits of accuracy of determining recovery). It can be seen that the ratio of radioactivity recovered in the different fractions is quite different between the cell lines. The LS-180 colon carcinoma cell line is known to produce an abundance of mucins (McCool *et al.*, 1995); the MDCK renal epithelial cells contain GPI-anchor glycoproteins (Nabi *et al.*, 1991; Zurzolo *et al.*, 1994) and proteoglycans (Svennevig *et al.*, 1995); the M-21 human melanoma cells are known to express abundant glycosphingolipids (Manzi *et al.*, 1990); and the CHO-K1 cells has been extensively used to study biosynthesis in various classes of glycans, including GAG chains (Esko, 1991).

We next examined the radioactivity in each final fraction to see if it indeed contained a major proportion of the predicted glycans. The PLE fractions which are expected to contain most of the GSLs were profiled by HPTLC, followed by detection with fluorography. Solvents appropriate for developing neutral GSLs or gangliosides were used. Such analyses showed that almost all the radioactivity in the PLE fractions from several cell lines migrated in positions expected for neutral and acidic glycolipids (data not shown). In all cases, there was very little radioactivity remaining at the origin (where free or peptide-bound glycans are expected to remain under these development conditions). The reproducibility of profiles obtained from the PLE preparation was also evident when comparing duplicates for each cell line, and the glycosphingolipid pattern is characteristic for each (see Figure 1 for examples). Further fractionation or structural characterization of these molecules was not done.

The add-back experiments in the preceding article (Manzi *et al.*, 2000) indicate that most of the GPI-anchors should be recovered in the secondary lipid extract (SLE fraction), still attached to an amino acid or a small peptide that survives the initial proteolysis. To confirm this for the metabolically labeled cells, we subjected this fraction to a standard protocol for release of neutral GPI core glycans (*Materials and*

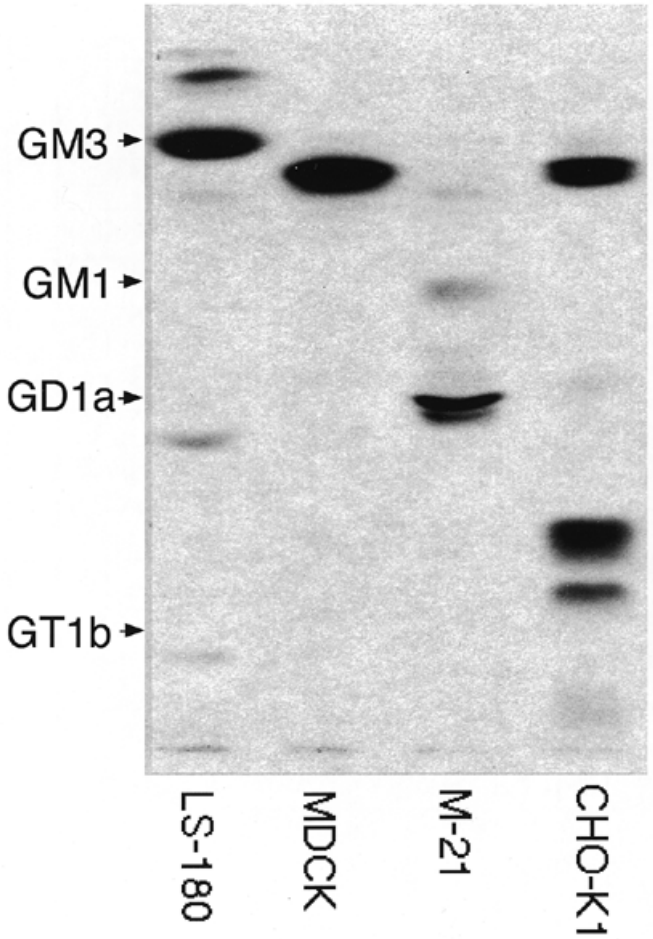

Fig. 1. HPTLC Profiling of total PLE fractions obtained from four different cultured cell lines metabolically radiolabeled with [6-^{3}H]GlcNH$_2$. The MDCK, M21, LS-180, and CHO cell lines were metabolically labeled with [6-^{3}H]GlcNH$_2$ and the radioactivity was separated into different fractions using the Glycan Isolation Protocol. Aliquots of the PLE fractions were subjected to HPTLC and bands detected by fluorography (*Materials and methods*).

methods), monitoring the radioactivity incorporated into the nonacetylated glucosamine residue in the GPI core region. As shown in the examples in Figure 2A, the radioactivity that bound to the HPAEC column (i.e., behaving as intact glycans), eluted in close proximity to the position of the glycan derived from the ^{3}H-labeled VSG GPI-glycan standard (the small variations in elution position could represent minor changes in the structure of the core glycan in different cell types). Although a major fraction of radioactivity ran through the column, this was seen in the standard as well, and represents degradation occurring during the steps of glycan release. Aliquots of the initial lipid extraction (PLE fractions) were also studied in a similar manner, looking for the presence of free (non protein-bound) glycosylinositol phospholipids (GIPLs). As shown in Figure 2B, a major peak that bound to the HPAEC column again eluted in the position expected for the GPI glycan product. This indicates that a significant fraction of the GPI glycans in cells are in the form of free GIPLs. To obtain a semi-quantitative view, we corrected the radioactivity recovered in the GPI glycan peak from the PLE and SLE fractions for the

Table II. Radioactivity recovered as [6-^{3}H]GlcN-labeled GPI-glycan in GIP lipids and GPI-anchors from four different cultured cell lines

Cell line	Radioactivity recovered in GPI-glycan		
	PLE (GIP Lipids)	SLE (GPI anchors)	Ratio GIPL/GPI
MDCK	163,813	62,757	2.6
M-21	141,918	38,816	3.6
LS-180	9,901	13,638	0.7
CHO-K1	155,742	42,594	3.7

Various cultured cell lines were metabolically labeled with [6-^{3}H]GlcN and the radioactivity was separated into different fractions using the Glycan Isolation Protocol. Aliquots of the PLE fractions and SLE fractions were treated with HF, HONO and borohydride reduction to release GPI-glycans, as described in *Materials and methods.* The glycans were then profiled by HPAEC. In each case, the amount of radioactivity recovered in the main GPI-glycan peak (see Figure for examples) was corrected for the fraction of input material.

fraction of input material. As shown in Table II, the ratio between the two is quite high in some cell lines. Even taking into account the ~50% recovery of standard GPI-anchors in the SLE fraction and the nearly 100% recovery for the standard GPI lipid obtained with the Glycan Isolation Protocol (see Manzi *et al.*, 2000), these ratios are still remarkably high. Overall, these data strongly support prior suggestions by others (Puoti and Conzelmann, 1992; Singh *et al.*, 1996; Ilgoutz *et al.*, 1999) that free GIP lipids may represent more than just a precursor pool for the new synthesis of GPI anchors in the ER. Indeed, we have shown here that in some cell types, the GIPLs may represent the majority of this class of molecules. Further work will be needed to pursue this observation. For example, an additional approach for quantitation would be the direct measurement of [^{3}H]anhydromannitol itself.

According to results in the preceding article (Manzi *et al.*, 2000), the $GP_{0–100}$ fraction should contain predominantly N- and O-glycan glycopeptides. Indeed, as shown in Figure 3, radioactivity released from these glycans by automated hydrazinolysis elutes in HPAEC chromatography in the regions expected for N- and O-glycans. Notably, each cell line has a distinct profile, which is reproducible between independent labelings. In each case, some of the label coelutes with typical mono- and di-sialylated core-2 type O-linked oligosaccharides (retention times of about 15 and 20 min, respectively). To confirm this, aliquots of the $GP_{0–100}$ fractions were submitted to automated hydrazinolysis using conditions optimized for the release and recovery of both N- and O-glycans, or just the O-glycans. This approach indicated that in addition to O-glycans, some of the peaks in the 10–20 min region are neutral and monosialylated N-glycans (data not shown). Some small labeled O-glycans were also found in the SLMW3 fraction as expected (data not shown).

The results in the preceding article indicate that the $GP_{100–1000}$ fraction should contain almost all of the GAG glycopeptides. Indeed, as shown in Figure 4, most of this radioactivity ran in the excluded volume of a FPLC size exclusion column, and a substantial portion was degraded into smaller fragments by a mixture of GAG-degrading enzymes. However, it is evident from Figure 4 that there was also a significant fraction resistant to degradation,

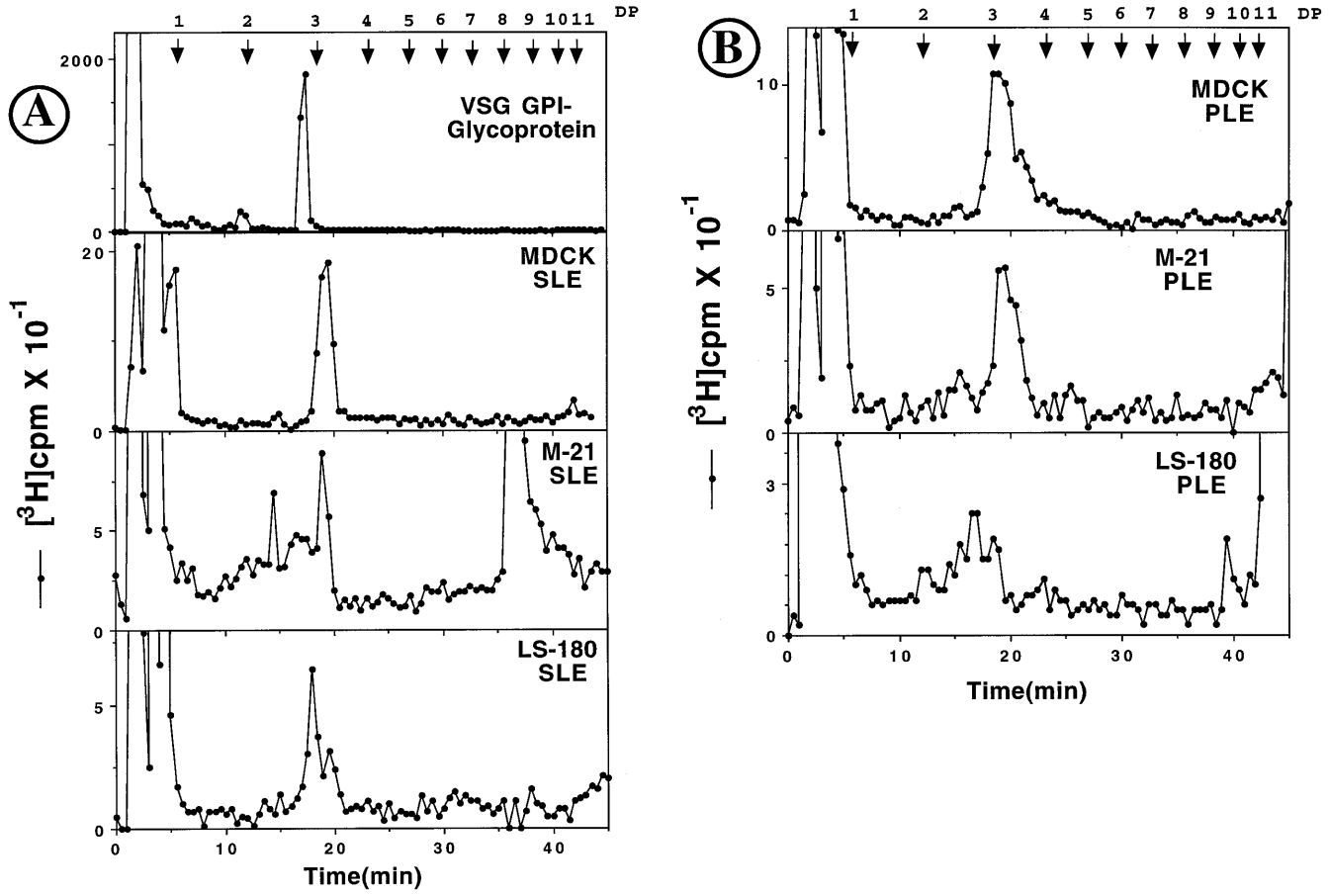

Fig. 2. Examples of HPAEC profiles of glycans released from the PLE and SLE fractions by HF treatment, nitrous acid deamination and reduction. The MDCK, M21, and LS-180 cell lines were metabolically labeled with [6-^{3}H]GlcN and subjected to the Glycan Isolation Protocol. Aliquots of (**A**) SLE and (**B**) PLE fractions were subjected to HF-treatment, nitrous acid deamination and reduction to release GPI-glycans (see Materials and methods). The released glycans were profiled by HPAEC in comparison to a standard GPI-glycan released from VSV-G.

especially in LS-180 cells. We considered the possibility that these were mucin-like glycopeptides carrying clustered sialylated O-glycans, which have a high charge density, and therefore do not elute from the DEAE column with 100 mM NaCl. Using labeled standards (see preceding article [Manzi *et al.*, 2000] for preparation) and carrying out elution steps with increasing concentrations of salt, we confirmed that an intermediate elution step with 300 mM NaCl elutes non-GAG mucin glycopeptide materials, before eluting GAGs with 1000 mM NaCl (Bame *et al.*, 1991). Indeed, the amount of this material can account for the material resistant to the mixture of GAG-degrading enzymes in the previous experiment. To verify this approach further, the subfraction $GP_{100-300}$ (300 mM elution after 100 mM elution) was studied from some of the metabolically labeled cell lines. As shown in Figure 5, when this fraction from CHO Pro-5 (wild-type) cells was subjected to automated hydrazinolyis (N- + O- mode) and studied by HPAEC profiling, the released molecules eluted mostly in the position of O-glycans. As shown in the lower panel of Figure 5, a similar profile was obtained with Lec1 mutant cells, which do not have any anionic N-glycans because of a processing defect (Stanley, 1992). Thus, the $GP_{100-300}$ fraction is indeed enriched in clustered O-glycans on mucin fragments.

Taken together, these data from metabolic labeling of several cultured cell lines confirm that each fraction derived from application of the Glycan Isolation Protocol does contain a major portion of the predicted classes of glycans. As discussed in the preceding paper, GAG chains with a low degree of sulfation and mucin-type glycopeptides with clustered anionic O-glycans have such similar charge density and charge/mass ratios that it is impossible to completely separate them based on physical principles alone.

Analysis of known mutants in N-glycan biosynthesis gives the expected changes in appropriate fractions

As an alternate approach to confirm that the different fractions contain the predicted classes of glycoconjugates, we studied several cell lines known to have specific defects in glycosylation pathways. In so doing, we also asked whether these biochemical defects would have been picked up if the Glycan Isolation Protocol had been used originally to analyze the cell lines.

We first compared a set of four cell lines, the parental CHO Pro-5, and some of its mutants: Lec1 (lacking GlcNAcT-I, and hence known to accumulate $Man_5GlcNAc_2Asn$ and lacking complex N-glycans), Lec2 (deficient in Golgi CMP-Sia transport and hence expected to lack Sia on GSLs, N-glycans and O-glycans), and Lec8 (deficient in Golgi UDP-Gal transport and hence expected to show major changes in almost all types of

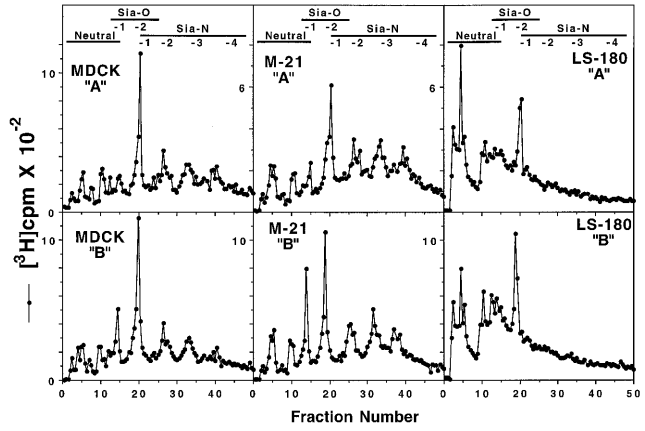

Fig. 3. HPAEC profiles of glycans from GP_{0-100} fractions. The MDCK, M21, and LS-180 cell lines were metabolically radiolabeled with [6-^{3}H]GlcN and subjected to the Glycan Isolation Protocol. Aliquots of the GP_{0-100} fractions were subjected to hydrazinolyis in the N-+O- mode and the released glycans were profiled by HPAEC. Examples of results are shown from cells metabolically radiolabeled with [6^3-H]GlcN on two separate occasions ("A" and "B"). The expected elution positions of neutral glycans, O-glycans with 1 or 2 sialic acids (Sia-O) or N-glycans with 1, 2, 3, or 4 sialic acids (Sia-N) are indicated.

Table III. Radioactivity metabolically incorporated from [6-^{3}H]GlcN and [^{35}S]sulfate into CHO-K1 and genetic variants altered in [^{35}S]sulfate incorporation: distribution into different fractions

Fraction	% of total radioactivity recovered					
	CHO-K1		pgsA-745		Clone 489	
	^{3}H	^{35}S	^{3}H	^{35}S	^{3}H	^{35}S
PLE	5.6	0	4.7	0	3.9	0
PLMW10	19.5	72.7	16.7	96.9	18.3	78.6
SLMW3	9.9	2.6	16.3	3.1	13.6	4.1
SLE	3.0	0	1.8	0	0.9	0
GP0-100	45.1	1.2	53.1	0	55.6	15.7
GP100–300	7.6	4.4	4.9	0	5.2	1.6
GP300–1000	7.2	18.2	0.4	0	0.4	0

The double-labeled cells were subjected to the Glycan Isolation Protocol and the radioactivity was monitored in each final fraction. See *Materials and methods* for the nomenclature of the fractions. For easy comparison the results are presented as percentage of total radioactivity recovered. The actual amount of [^{35}S]sulfate incorporation was highest in the wild-type cells and lowest in pgsA-745, with clone 489 giving intermediate values.

glycoconjugates). Some differences were observed in the distribution of radioactivity amongst various fractions, including a reduction in the GP_{0-100} fractions in all the mutants, and a relative increase in the $GP_{100-1000}$ fraction of Lec1 cells (data not shown). This is presumably because of a decrease in GlcNAc incorporation into N-glycans in Lec1 cells, and a relative lack of sialic acid incorporation in all three mutant cell lines. As shown in Figure 6, the glycans released by automated hydrazinolysis in the N- + O- mode show marked changes in HPAEC profiling, due to varying degrees of blockage in processing to fully branched sialylated forms. As expected, complex N-linked

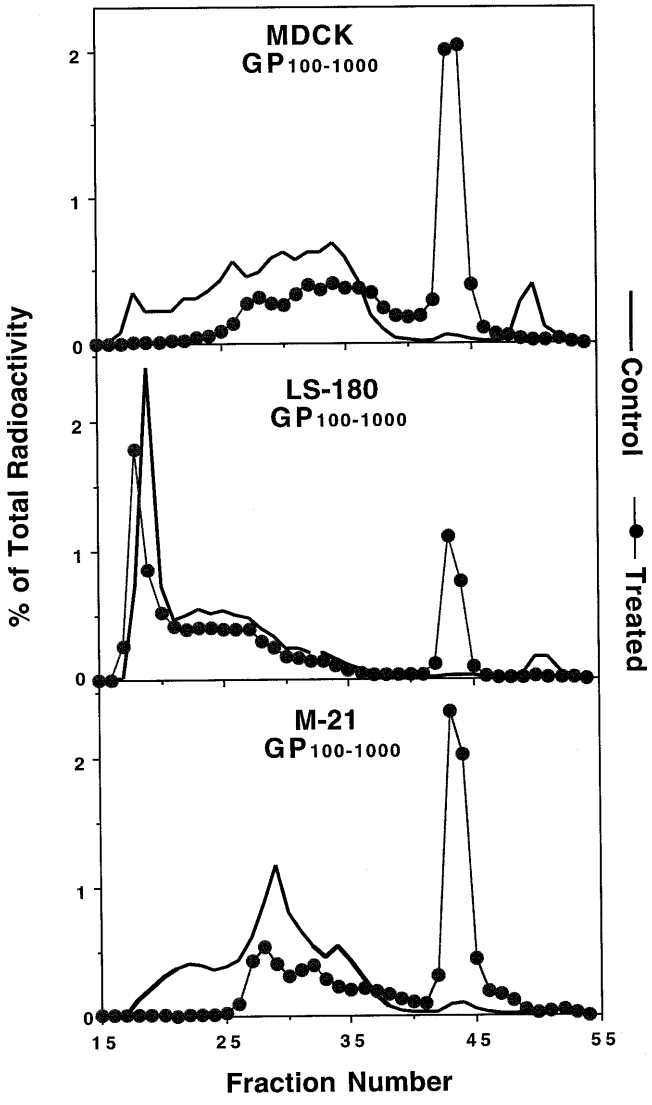

Fig. 4. Size exclusion chromatography of the $GP_{100-1000}$ fractions: effects of GAG-degrading enzymes. The MDCK, M21, and LS-180 cell lines were metabolically labeled with [6-^{3}H]GlcN and subjected to the Glycan Isolation Protocol. Aliquots of the $GP_{100-1000}$ fractions were analyzed by S-12 HPLC size exclusion chromatography with and without prior treatment with a mixture of GAG-degrading enzymes. Column V_t = fractions 16–18, V_0 = fractions 52–54.

chains are practically absent in Lec1 and both N- and O-linked glycans are affected by the lack of transport of CMP-Sia and UDP-Gal into the Golgi (Lec2 and Lec8, respectively). In the last two cases, complete absence of the mucin-type clustered anionic O-glycans in a $GP_{100-300}$ fraction was also observed (data not shown). To further assure reproducibility, we also studied clone 1021, an independent CHO mutant which, like Lec8, is deficient in the transport of UDP-Gal into the Golgi. The N- and O-glycan profiles were indeed similar to those of Lec8 (data not shown). Lec2 and Lec8 cells also showed some increase in recovered radioactivity in the SLMW3 fraction (50% and 100% increase, respectively). This is probably because O-glycans fail to get sialylated/galactosylated, and the resulting small neutral glycopeptides pass through the 3000 MW cut-off membrane during the first ultrafiltration step.

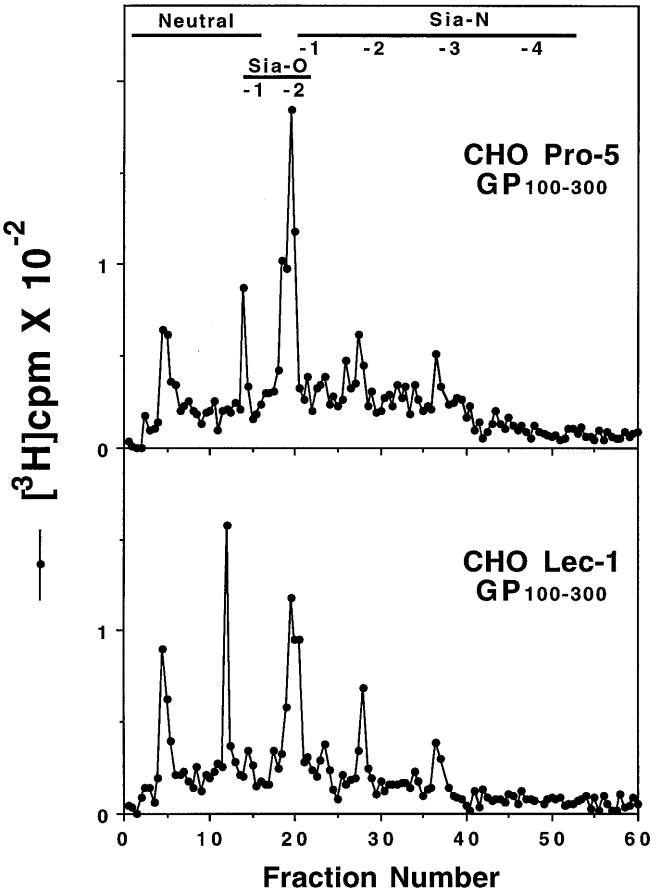

Fig. 5. HPAEC profiles of glycans from $GP_{100-300}$ fractions of two metabolically labeled cultured cell lines. The CHO Pro5 and Lec1 cell lines were metabolically labeled with [6-^{3}H]GlcN and subjected to the Glycan Isolation Protocol. The 300 mM DEAE elution step was included, generating $GP_{100-300}$ fractions. Aliquots of these fractions were subjected to automated hydrazinolysis in the "N- + O" mode and the released glycans were profiled by HPAEC. The markers indicate the expected elution positions of O-glycans with one or two sialic acids (Sia-O) or N-glycans with 1, 2, 3, or 4 sialic acids (Sia-N). Similar results were obtained with samples subjected to automated hydrazinolysis in the O-glycan release mode (data not shown).

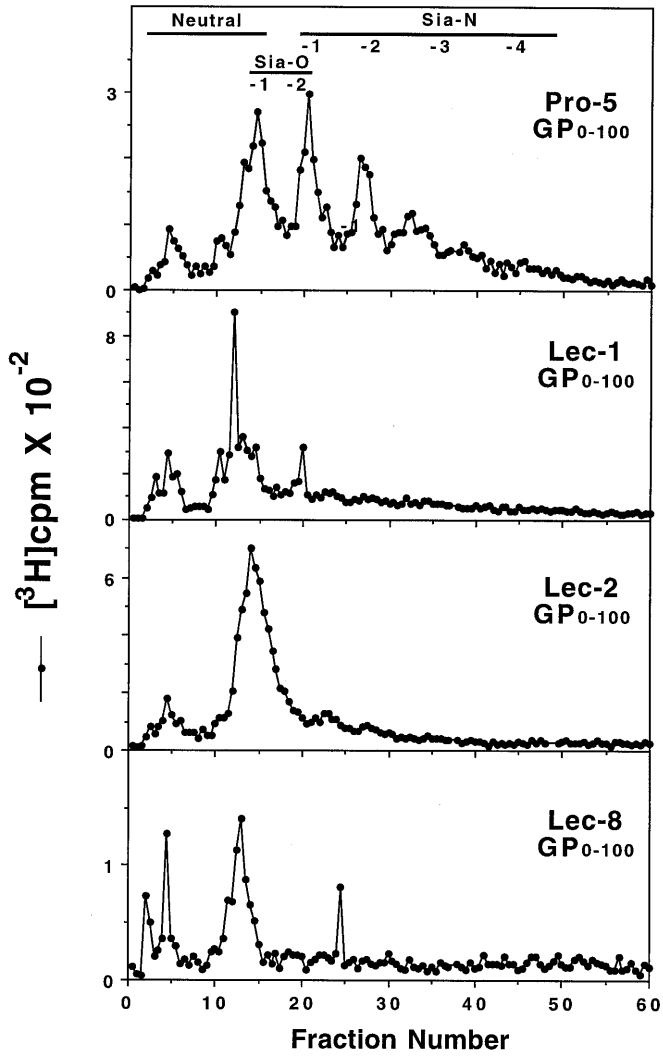

Fig. 6. HPAEC profiles of metabolically radiolabeled glycans from the GP_{0-100} fractions. The CHO Pro-5, Lec1, Lec2, and Lec8 cell lines were metabolically labeled with [6-^{3}H]GlcN and subjected to the Glycan Isolation Protocol. Aliquots of the GP_{0-100} fractions were subjected to hydrazinolyis in the N-+O-mode and the released glycans profiled by HPAEC. The upper panel also notes the expected position of elution of standard N- and O-glycans, indicated as in Figure 3.

Analysis of known mutants in GAG chain biosynthesis

We compared the CHO-K1 parental line with the mutant cell lines pgsA-745 (lacking the UDP-Xylose:core protein β-xylosyltransferase, resulting in a complete block in all GAG biosynthesis), and pgsD-677 (deficient in the UDP-GlcNAc/UDP-GlcA heparan copolymerase, and thereby selectively lacking heparan sulfate chains). The total glycopeptides were applied to the DEAE column and eluted in three steps, including the intermediate 300 mM NaCl step to ensure that mucin-type glycopeptides are separated from HS and CS GAG chains. As expected, CHO pgsA-745 cells showed an almost complete loss of incorporation of radioactivity into the fraction $GP_{300-1000}$ (eluted with 1M NaCl), confirming the predicted loss of CS and HS chains (Table III). However, the same fraction showed only a small reduction in incorporated radioactivity in the mutant pgsD-677, which lacks HS chains, but still expresses CS chains (data not shown). Without prior knowledge of the defect in this line, this screening method might have missed this difference. However, when aliquots of the $GP_{300-1000}$ fractions from the wild-type and pgsD-677 mutant are treated with the various GAG-degrading enzymes and analyzed for size on a Superose-12 FPLC column (Figure 7), the alteration in the mutant became evident. The largest population of molecules from the wild-type CHO-K1 cells are primarily digested by the chondroitinases, and the population in fractions 30–35 comprises the heparan-type GAGs susceptible to heparin lyase II. In contrast, the pgsD-677 profiles show no major shift in size following heparanase digestion, and the starting material elutes between fractions 19 and 30, where the CS from the parental cell line elutes. Overall, these data indicate that when using it to screen for mutants, the isolation protocol needs to be accompanied by profiling analyses.

Changes in profiles of some other glycan classes in various mutant cell lines

Ganglioside biosynthesis is also affected in some of the mutant cells. HPTLC analysis of the PLEs from Pro-5, Lec1, Lec2,

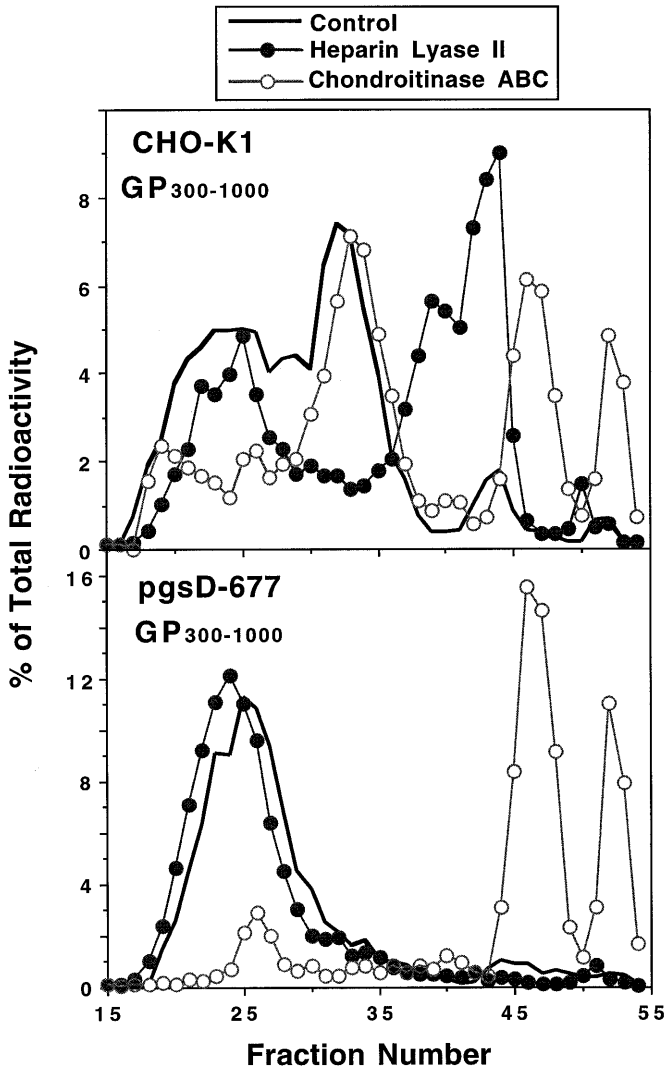

Fig. 7. Size exclusion chromatography of the $GP_{300-1000}$ fractions: effects of GAG-degrading enzymes. CHO-K1 and its mutant pgsD-677 were metabolically labeled with [6-^{3}H]GlcN and subjected to the Glycan Isolation Protocol. Aliquots of the $GP_{300-1000}$ fractions were analyzed by S-12 HPLC size exclusion chromatography with and without prior treatment with specific GAG-degrading enzymes as indicated. Column V_t = fractions 16–18, V_0 = fractions 52–54.

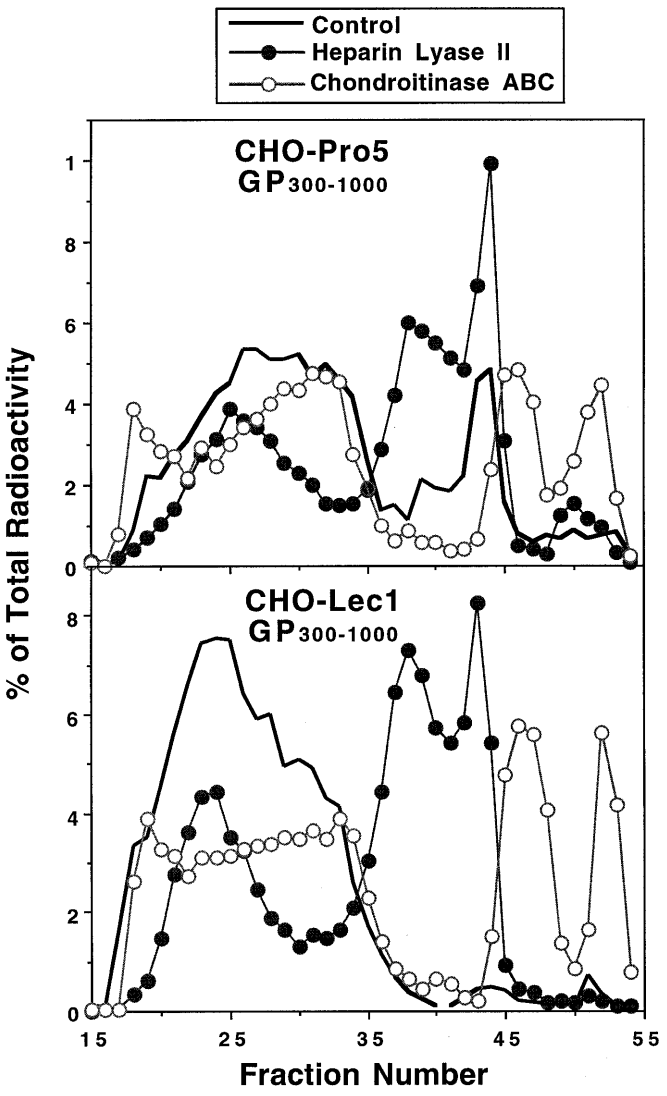

Fig. 8. Size exclusion chromatography of the GP300–1000 fractions: effects of GAG-degrading enzymes. CHO-Pro-5 parent cell line and its mutant Lec 1 were metabolically labeled with [6-^{3}H]GlcN and subjected to the Glycan Isolation Protocol. Aliquots of the $GP_{300-1000}$ fractions were analyzed by S-12 HPLC size exclusion chromatography with and without prior treatment with specific GAG-degrading enzymes as indicated. Column V_t = fractions 16–18, V_0 = fractions 52–54.

and Lec8 indicated some reproducible differences (data not shown). G_{M3}, a major component of the PLE in Pro-5 and Lec1, is not found in Lec2 and Lec8, as expected from the lack of availability of precursors (UDP-Gal, CMP-Neu5Ac) required to synthesize this molecule. The GAG-digestion profiles of the Pro-5 parental cell line and three of its mutants showed some surprising differences. Notably, Lec1 cells express a GAG population (sensitive to combined digestion with heparin lyase II and Chondroitinase ABC, not shown) that is skewed to a substantially larger size (Figure 8), and the smaller fragments seen in the wild-type cells were not present (there was no difference in the percentage distribution of radioactivity into this fraction). Also, while some of the material from all of the cell lines is susceptible to heparin lyase II, the ratios of the two smaller peaks (fractions 36–41 and 42–45) produced are different (see Figure 8). Furthermore, while some of the material from all cell lines is susceptible to chondroitinase ABC, Lec-1 has more material susceptible to this enzyme. These experiments indicate that changes in some classes of glycans can be seen that are not necessarily predicted by the primary defect (in this case, GlcNAcT-I deficiency, a defect in N-glycan biosynthesis apparently results in a change in the size of GAGs).

Generation and analysis of a novel CHO cell line with restored sulfation

The mutant cell line pgsA-745 fails to incorporate significant amounts of [^{35}S]sulfate, because it is completely deficient in the xylosyltransferase that initiates HS and CS GAG chain synthesis (Esko *et al.*, 1985). These cells were transfected with a cDNA library from wild-type CHO cells, and screened for restoration of [^{35}S]sulfate incorporation into TCA-precipitable

products. Two such lines (clone 489 and 26) obtained by this approach showed an increase in [^{35}S] incorporation. Both of these gave very similar results, indicating that they are either closely related, or actual sibling clones (Bai *et al.*, unpublished observations). Clone 489 cells were double-labeled with [^{3}H]GlcN and [^{35}S]sulfate and characterized by the Glycan Isolation Protocol, to see if GAG chain synthesis had been restored. However, as shown in Table III, label incorporation was not restored as expected in the $GP_{300–1000}$ fraction, where GAG glycopeptides are found. Instead, the "restored" label was almost exclusively in the $GP_{0–100}$ and $GP_{100–300}$ fractions where N- and O-linked glycopeptides are expected to be recovered. The lack of restored sulfation in any other fraction makes it very likely that a new enzymatic activity has been introduced into the cells, which results in increased sulfation of pre-existing N-glycans and/or O-glycans. Further characterization of this mutant is under way.

Conclusions and perspectives

We have applied the Glycan Isolation Protocol described in the preceding article (Manzi *et al.*, 2000) to study cultured cell lines and their glycosylation mutants. By metabolically radiolabeling with [6-^{3}H]glucosamine, we were able to monitor the nature and recovery of each class of glycans. These results allow us to reach several conclusions that enhance and complement those obtained from the previous paper (Manzi *et al.*, 2000). We found good recovery of total radioactivity and the distribution of label to be largely in the correct glycan classes in fractions from a variety of cell lines. One unexpected finding was that the amount of radioactivity recovered in free glycosylphosphatidylinositol lipids (GIPLs) is quite high when compared with that found in GPI anchors in the same cells. Indeed, the free lipid form appears to be the dominant one in some cells (e.g., CHO-K1 and M21 cells). It is difficult to imagine that all of this simply represents an ER precursor pool awaiting conversion to GPI-anchors. It appears more likely that these are true free GIPLs, such as those recently suggested by other investigators (Puoti and Conzelmann, 1992; Singh *et al.*, 1996). Further studies of the topology (inner versus outer leaflet) and the subcellular distribution (e.g., how much is actually in the ER?) of this GIPL fraction seem to be warranted.

We also demonstrate that the radiolabeled fractions obtained are of sufficient quality to show the expected change in cells with known genetic mutations in specific glycosylation pathways as well as to examine other classes of glycans for unexpected changes. Furthermore, we note that some mutants show unexpected changes in the profiles of glycan classes that are not predicted to be affected by the primary defect. Finally, we used this protocol to demonstrate that the reappearance of sulfation in the transfected clone 489 is apparently not due to simple restoration of GAG sulfation, but rather due to the *de novo* expression of sulfation in the $GP_{0–100}$ and $GP_{100–300}$ fractions (which are expected to contain mostly N- and O-linked glycopeptides). Overall, these results demonstrate the power of this comprehensive approach for the concurrent exploration and profiling of the different major classes of glycans in vertebrate cells.

Materials and methods

Materials

Most of the materials used were obtained from the Sigma Chemical Company and/or are listed in the preceding article (Manzi *et al.*, 2000). [^{3}H] 2,5-anhydromannitol was generated from [6-^{3}H]-GlcN or GlcN hydrochloride by nitrous acid deamination followed by reduction with $NaB[^{3}H]_4$. All other chemicals were of reagent grade or better, and were obtained from commercial sources.

Cell lines and metabolic radiolabeling

The CHO cell lines Lec1, Lec2, and Lec8 (originally produced by Pamela Stanley and colleagues) and the wild-type originals K1 and Pro-5 were obtained from ATCC (Stanley, 1992; Stanley and Ioffe, 1995). The CHO Clone 1021 (Briles *et al.*, 1977) was kindly provided by Stuart Kornfeld, Washington University, St. Louis. The pgsA-745 and pgsD-677 lines were derived from CHO-K1 cells in the laboratory of one of us (J.E.) (Esko *et al.*, 1985; Lidholt *et al.*, 1992). The new CHO line 489 was derived from the GAG-deficient line pgsA-745 by transfection with a wild-type CHO-K1 cDNA library, and subsequent selection for restoration of [^{35}S]sulfate incorporation (by replica-filter detection). Details concerning the production of this cell line will be described elsewhere. Cell monolayers were metabolically radiolabeled with [6-^{3}H]GlcN and/or with [^{35}S]sulfate as described in the preceding paper (Manzi *et al.*, 2000). Under these conditions, most of the label from [6-^{3}H]glucosamine should remain in various glycan classes, but some can potentially enter into non-carbohydrate molecules.

Isolation of different classes of glycans from metabolically radiolabeled cells

After aspiration of the radioactive media, cells were washed three times with cold PBS, scraped off the plate, recovered by centrifugation, and the pellet was subjected to total lipid extraction exactly as described in the preceding article (Manzi *et al.*, 2000). The extracellular matrix left behind on the plate was solubilized with 1% SDS/100 mM Tris-Cl, pH 7.4, at room temperature (RT) for 5–10 min, with further scraping. The solubilized ECM was combined with the protein fraction obtained after the initial extraction of total lipids, and heated for 10 min at 100°C with vortexing. The SDS-solubilized extract was submitted to the complete Glycan Isolation Protocol essentially as described in the preceding article (Manzi *et al.*, 2000), with β-counting used to monitor the recoveries. The nomenclature of the different fractions isolated by the Glycan Isolation Protocol is identical to that in the preceding article (Manzi *et al.*, 2000). TH, total homogenate obtained after the initial homogenization of the sample in organic solvents. PLE, primary lipid extract, obtained after removing all material insoluble in organic solvents. TP, total glycoproteins and proteoglycans, after solubilization of the delipidated pellet in SDS. PLMW10, primary low molecular weight fraction obtained by ultrafiltration of the SDS extract against a 10,000 MW cutoff membrane. TGP, total glycopeptides, after Proteinase K digestion, before ultrafiltration. SLMW3, secondary low molecular weight fraction obtained by ultrafiltration of the Proteinase K digest against a 3000 MW cutoff membrane. SLE, secondary lipid extract, obtained by organic extraction after SDS precipitation. GP_U, total unfrac-

tionated glycopeptides, after secondary organic extraction, before DEAE. GP_{0-100}, glycopeptides running through/eluting from DEAE in 100mM NaCl. $GP_{100-1000}$, glycopeptides eluting from DEAE in 1000 mM NaCl after 100 mM NaCl elution. $GP_{100-300}$, glycopeptides eluting from DEAE in 300 mM NaCl after 100 mM NaCl elution. $GP_{300-1000}$, glycopeptides eluting from DEAE in 1000 mM NaCl after 300 mM NaCl elution.

Conventional isolation of glycosylphosphatidyl-inositol (GPI)-anchored proteins

Some of the cell lines were submitted to the classical protocol for the isolation of the GPI-anchored proteins (Doering *et al.*, 1996). Briefly, Triton X-114 was pre-condensed and added (~2% final conc.) to cell suspensions in ice-cold TBS to a final protein concentration of ~<4 mg/ml in a 15 ml tube. The mixture was incubated for 10 min on ice with occasional stirring. The one-phase supernatant obtained by centrifugation (10 min at 10,000 × *g*, 4°C) was transferred to a fresh tube and the pellet resuspended in ice-cold TBS. The supernatant was warmed to 37°C until the solution became cloudy, centrifuged in a tabletop centrifuge (10 min at 1000 × *g*, RT), and the upper and lower phases were collected into separate tubes. The GPI-anchor-enriched fraction is the lower phase.

Release of N- and O-linked glycans from glycopeptides by automated hydrazinolysis

This was done as described in the preceding article (Manzi *et al.*, 2000).

Generation of core plycans from GPI-type glycopeptides

The presence of GPI-glycans metabolically labeled with [^{3}H]GlcN can be determined by detecting the ^{3}H-labeled glycan bearing labeled 2,5-anhydromannitol, which is generated by nitrous acid (HONO) deamination and reduction of the unsubstituted GlcN residue present in such glycans (Ferguson, 1992). Thus, ^{3}H-labeled GPI-anchor glycopeptides (in the SLE fraction) and free ^{3}H-labeled GPI-lipids (in the PLE fraction) were deacylated, dephosphorylated, deaminated and reduced as described (Menon *et al.*, 1990). Briefly, the dry samples were deacylated with 30% NH_4OH in methanol (1:1 v/v) for 2 h at 37°C and dried. Dephosphorylation was then done with 50% aqueous HF for 60 h in a Dewar flask bathed in an ice-water mixture, and the HF was volatilized under a stream of nitrogen. The sample was dissolved in water, desalted over Dowex AG 3-X4 (OH-), and dried again. Nitrous acid deamination was then done with 0.25 M $NaNO_2$ freshly prepared in 0.2 M sodium acetate (pH 3.7), at RT for 4 h. The reaction was terminated by adding 300 µl of 0.4 M boric acid, and the glycans liberated from the lipid were recovered in the aqueous phase after butanol/water phase partitioning. After adjusting the pH to 10 with NaOH, the samples were reduced with sodium borohydride or borotritide as appropriate, and desalted over Dowex AG 50W-X12 (H^+ form). Methyl borates were eliminated by evaporation from 5% acetic acid in methanol four times and residual acetic acid removed by evaporation with added toluene.

HPTLC profiling of neutral GSLs and gangliosides (Schnaar and Needham, 1994)

Dry PLEs were dissolved in the minimum possible volume of $CHCl_3$:MeOH (2:1, v/v). Glass coated Silica Gel-60 HPTLC plates (10 × 10 cm)were activated for 20 min at 110°C. Aliquots of each sample (~25,000 c.p.m.) were spotted on two different plates: one was developed with $CHCl_3$:MeOH:water (70:30:4, v/v/v) for the separation of neutral GSL species; the second with $CHCl_3$:MeOH:0.2M $CaCl_2$ (60:40:9, v/v), for separation of acidic GSLs. Radiolabeled GSLs were detected by spraying HPTLC plates with En^{3}Hance (DuPont-New England Nuclear), and fluorography, and migration compared with unlabeled standards.

HPAEC oligosaccharide profiling

For N- and O-glycans released by hydrazinolysis from fractions SLMW3, GP_{0-100}, and $GP_{100-300}$, profiling was done essentially as described previously (Manzi *et al.*, 2000) Neutral core glycans from GPIs containing [^{3}H]2,5-anhydromannitol or free [^{3}H]2,5-anhydromannitol released by TFA hydrolysis were analyzed by HPAEC using a PA-1 column eluted with a linear gradient of sodium acetate from 0 to 75 mM with constant sodium hydroxide concentration (100 mM). Fractions (0.5 min) were collected and monitored by β-counting. The elution position of unlabeled standards was detected by PAD.

Analysis of glycosaminoglycan content

The presence and type of glycosaminoglycans (GAGs) was assessed by the susceptibility of various fractions to GAG degrading enzymes. Samples were dissolved in 50 mM Tris-Acetate (pH 7.0), containing 2.5 mM $CaCl_2$ and 100 mM NaCl and enzymes added as required: heparan sulfate was detected with 750 mU heparin lyase II; chondroitin sulfate with 60 mU chondroitinase ABC; and keratan sulfate with 160 mU keratanase I and 4 mU keratanase II. The reaction mixtures were incubated overnight at 37°C, boiled for 10 min and applied to a Pharmacia Superose 12 HR 10/30 FPLC column to size undigested and digested products. The column was run isocratically in 125 mM NaCl/20 mM HEPES (pH 7.4), containing 0.02% sodium azide. A Pharmacia FPLC system (P-LKB-Pump P-500; P-LKB-Controller LCC-500 Plus) was used to elute the column at 0.4 ml/min flow rate. Fractions were monitored for radioactivity.

Acknowledgments

We thank Herman van Halbeek for his review of the manuscript, and Delia Matriano for expert technical help. This work was supported by USPHS Grants P01 HL57345 (A.V.) and R01 GM33063, (J.E.), and by the G.Harold & Leila Y.Mathers Charitable Foundation.

Abbreviations

CHO, Chinese hamster ovary; CS, chondroitin sulfate; DS, dermatan sulfate; GAG, glycosaminoglycan with a Xyl residue O-linked to Ser; GIPL, glycosylinositol phospholipid; GPI, glycosylphosphatidyl-inositol; GPI-anchors, glycophosphatidylinositol anchors; GSLs, glycosphingolipids; Cer, ceramide; HF, hydrogen fluoride; HPAEC, high pH anion-exchange chromatography; HPLC, high performance liquid chromatography; HPTLC, high performance thin layer chromatography; HS, heparan sulfate; KS, keratan sulfate; N-glycans, oligosaccharides with GlcNAc N-linked to Asn; O-glycans, oligosac-

charides with GalNAc O-linked to Ser/Thr; TBS, Tris-buffered saline; TFA, trifluoroacetic acid; VSG, variable surface glycoprotein.

References

Abeijon,C., Mandon,E.C. and Hirschberg,C.B. (1997) Transporters of nucleotide sugars, nucleotide sulfate and ATP in the Golgi apparatus. *Trends Biochem. Sci.*, **22**, 203–207.

Bai,X.M. and Esko,J.D. (1996) An animal cell mutant defective in heparan sulfate hexuronic acid 2-O-sulfation. *J. Biol. Chem.*, **271**, 17711–17717.

Bai,X.M., Wei,G., Sinha,A. and Esko,J.D. (1999) Chinese hamster ovary cell mutants defective in glycosaminoglycan assembly and glucuronosyltransferase I. *J. Biol. Chem.*, **274**, 13017–13024.

Bame,K.J., Reddy,R.V. and Esko,J.D. (1991) Coupling of *N*-deacetylation and *N*-sulfation in a Chinese hamster ovary cell mutant defective in heparan sulfate *N*-sulfotransferase. *J. Biol. Chem.*, **266**, 12461–12468.

Briles,E.B., Li,E. and Kornfeld,S. (1977) Isolation of wheat germ agglutinin-resistant clones of Chinese hamster ovary cells deficient in membrane sialic acid and galactose. *J. Biol. Chem.* **252**, 1107–1116.

Dinter,A. and Berger,E.G. (1998) Golgi-disturbing agents. *Histochem. Cell Biol.*, **109**, 571–590.

Doering,T.L., Englund,P.T. and Hart,G.W. (1996) Detection of glycophospholipid anchors on proteins. In Ausubel,F.M., Brent,R., Kingston,R.E., Moore,D.D., Seidman,J.G., Smith,J.A., Struhl,K., Albright,L.M., Coen,D.M. and Varki,A. (eds.), *Current Protocols in Molecular Biology.* John Wiley & Sons, New York, pp. Unit 17–8.

Esko,J.D., Stewart,T.E. and Taylor,W.H. (1985) Animal cell mutants defective in glycosaminoglycan biosynthesis. *Proc. Natl Acad. Sci. USA*, **82**, 3197–3201.

Esko,J.D. (1986) Detection of animal cell LDL mutants by replica plating. *Methods Enzymol.*, **129**, 237–253.

Esko,J.D. (1989) Replica plating of animal cells. *Methods Cell Biol.*, **32**, 387–422.

Esko,J.D. (1991) Genetic analysis of proteoglycan structure, function and metabolism. *Curr. Opin. Cell Biol.*, **3**, 805–816.

Ferguson,M.A.J. (1992) Lipid anchors on membrane proteins. *Curr. Opin. Struct. Biol.*, **1**, 522–529.

Furukawa,K. and Kobata,A. (1992) Protein glycosylation. *Curr. Opin. Biotechnol.*, **3**, 554–559.

Gottlieb,C., Skinner,A.M. and Kornfeld,S. (1974) Isolation of a clone of Chinese hamster ovary cells deficient in plant lectin-binding sites. *Proc. Natl. Acad. Sci. USA*, **71**, 1078–1082.

Hart,G.W. (1992) Glycosylation. *Curr. Opin. Cell Biol.*, **4**, 1017–1023.

Hart,G.W. (1997) Dynamic O-linked glycosylation of nuclear and cytoskeletal proteins. *Annu. Rev. Biochem.*, **66**, 315–335.

Hascall,V.C., Calabro,A., Midura,R.J. and Yanagishita,M. (1994) Isolation and characterization of proteoglycans. *Methods Enzymol.* **230**, 390–417.

Hayes,B.K. and Hart,G.W. (1994) Novel forms of protein glycosylation. *Curr. Opin. Struct. Biol.*, **4**, 692–696.

Ilgoutz,S.C., Zawadzki,J.L., Ralton,J.E. and McConville,M.J. (1999) Evidence that free GPI glycolipids are essential for growth of *Leishmania mexicana*. *EMBO J.*, **18**, 2746–2755.

Lidholt,K., Weinke,J.L., Kiser,C.S., Lugemwa,F.N., Bame,K.J., Cheifetz,S., Massagué,J., Lindahl,U. and Esko,J.D. (1992) A single mutation affects both *N*-acetylglucosaminyltransferase and glucuronosyltransferase activities in a Chinese hamster ovary cell mutant defective in heparan sulfate biosynthesis. *Proc. Natl. Acad. Sci. USA*, **89**, 2267–2271.

Lis,H. and Sharon,N. (1993) Protein glycosylation—structural and functional aspects. *Eur. J. Bioche m.*, **218**, 1–27.

Manzi,A.E., Sjoberg,E.R., Diaz,S. and Varki,A. (1990) Biosynthesis and turnover of *O*-acetyl and *N*-acetyl groups in the gangliosides of human melanoma cells. *J. Biol. Chem.*, **265**, 13091–13103.

Manzi,A.E., Norgard-Sumnicht,K., Argade,S., Marth,J.D., van Halbeek,H. and Varki,A. (2000) Exploring the glycan repertoire of genetically modified mice by isolation and profiling of the major glycan classes and nano-NMR analysis of glycan mixtures. *Glycobiology,* **10**, 669–689.

Margolis,R.K. and Margolis,R.U. (1993) Nervous tissue proteoglycans. *Experientia*, **49**, 429–446.

McCool,D.J., Forstner,J.F. and Forstner,G.G. (1995) Regulated and unregulated pathways for MUC2 mucin secretion in human colonic LS180 adenocarcinoma cells are distinct. *Biochem. J.*, **312**, 125–133.

Menon,A.K., Schwarz,R.T., Mayor,S. and Cross,G.A.M. (1990) Cell-free synthesis of glycosyl-phosphatidylinositol precursors for the glycolipid membrane anchor of Trypanosoma brucei variant surface glycoproteins. Structural characterization of putative biosynthetic intermediates. *J. Biol. Chem.*, **265**, 9033–9042.

Nabi,I.R., Le Bivic,A., Fambrough,D. and Rodriguez-Boulan,E. (1991) An endogenous MDCK lysosomal membrane glycoprotein is targeted basolaterally before delivery to lysosomes. *J. Cell Biol.*, **115**, 1573–1584.

Potvin,B., Raju,T.S. and Stanley,P. (1995) *lec32* is a new mutation in Chinese hamster ovary cells that essentially abrogates CMP-*N*-acetylneuraminic acid synthetase activity. *J. Biol. Chem.*, **270**, 30415–30421.

Puoti,A. and Conzelmann,A. (1992) Structural characterization of free glycolipids which are potential precursors for glycophosphatidylinositol anchors in mouse thymoma cell lines. *J. Biol. Chem.*, **267**, 22673–22680.

Roseman,S. (1970) The synthesis of carbohydrates by multiglycosyltransferase systems and their potential function in intercellular adhesion. *Chem. Phys. Lipids*, **5**, 270–297.

Sadler,J.E., Beyer,T.A., Oppenheimer,C.L., Paulson,J.C., Prieels,J.P., Rearick,J.I. and Hill,R.L. (1982) Purification of mammalian glycosyltransferases. *Methods Enzymol.*, **83**, 458–514.

Schachter,H. (1991) The "yellow brick road" to branched complex N-glycans. *Glycobiology*, **1**, 453–462.

Schnaar,R.L. (1991) Glycosphingolipids in cell surface recognition. *Glycobiology*, **1**, 477–485.

Schnaar,R.L. and Needham,L.K. (1994) Thin-layer chromatography of glycosphingolipids. *Methods Enzymol.*, **230**, 371–389.

Singh,N., Liang,L.N., Tykocinski,M.L. and Tartakoff,A.M. (1996) A novel class of cell surface glycolipids of mammalian cells—free glycosyl phosphatidylinositols. *J. Biol. Chem.*, **271**, 12879–12884.

Stanley,P. (1984) Glycosylation mutants of animal cells. *Annu. Rev. Genet.*, **18**, 525–552.

Stanley,P. (1992) Glycosylation engineering. *Glycobiology*, **2**, 99–107.

Stanley,P. and Ioffe,E. (1995) Glycosyltransferase mutants: key to new insights in glycobiology. *FASEB J.*, **9**, 1436–1444.

Stanley,P., Raju,T.S. and Bhaumik,M. (1996) CHO cells provide access to novel *N*-glycans and developmentally regulated glycosyltransferases. *Glycobiology*, **6**, 695–699.

Svennevig,K., Prydz,K. and Kolset,S.O. (1995) Proteoglycans in polarized epithelial Madin-Darby canine kidney cells. *Biochem. J.*, **311**, 881–888.

Van den Eijnden,D.H. and Joziasse,D.H. (1993) Enzymes associated with glycosylation. *Curr. Opin. Struct. Biol.*, **3**, 711–721.

Van den Eijnden,D.H., Neeleman,A.P., Van der Knaap,W.P.W., Bakker,H., Agterberg,M. and Van Die,I. (1995) Novel glycosylation routes for glycoproteins: the lacdiNAc pathway. *Biochem. Soc. Trans.*, **23**, 175–179.

Varki,A. (1994) Metabolic radiolabeling of glycoconjugates. *Methods Enzymol.*, **230**, 16–32.

Varki,A. and Freeze,H.H. (1994) The major glycosylation pathways of mammalian membranes; a summary. In Maddy,A.H. and Harris,J.R. (eds.), *Subcellular Biochemistry.* Plenum Press, New York, pp. 71–100.

Varki,A. (1998) Factors controlling the glycosylation potential of the Golgi apparatus. *Trends Cell Biol.* **8**, 34–40.

Weigel,P.H., Hascall,V.C. and Tammi,M. (1997) Hyaluronan synthases. *J. Biol. Chem.*, **272**, 13997–14000.

Yeh,J.C. and Cummings,R.D. (1997) Differential recognition of glycoprotein acceptors by terminal glycosyltransferases. *Glycobiology*, **7**, 241–251.

Zhang,A.M., Potvin,B., Zaiman,A., Chen,W., Kumar,R., Phillips,L. and Stanley,P. (1999) The gain-of-function Chinese hamster ovary mutant LEC11B expresses one of two Chinese hamster *FUT6* genes due to the loss of a negative regulatory factor. *J. Biol. Chem.*, **274**, 10439–10450.

Zurzolo,C., Van't Hof,W., van Meer,G. and Rodriguez-Boulan,E. (1994) VIP21/caveolin, glycosphingolipid clusters and the sorting of glycosylphosphatidylinositol-anchored proteins in epithelial cells. *EMBO J.*, **13**, 42–53.